Research Article

Long Yang*#, Na Deng#, Jionghong He#, Guiling Xia, Ying Yang, Yidong Zhao, Zhaomei Huo, Chuxian Guo

Calcineurin Aβ gene knockdown inhibits transient outward potassium current ion channel remodeling in hypertrophic ventricular myocyte

https://doi.org/10.1515/biol-2021-0107
received April 07, 2021; accepted August 16, 2021

Abstract: It has been shown that the activation of calcineurin is involved in regulating ion channel remodeling in hypertrophic cardiomyocytes. But the precise role of calcineurin in the regulation of transient outward potassium current (I_{to}), an ion channel associated with fatal arrhythmia, remains controversial. This study aimed to examine the effects of *calcineurin Aβ* (*CnAβ*) gene knockdown on I_{to} channel remodeling and action potential duration (APD) in the hypertrophic ventricular myocytes of neonatal rats. Results showed that phenylephrine stimulation caused hypertrophy of ventricular myocytes, upregulation of CnAβ protein expression, downregulation of *Kv4.2* mRNA and protein expression, a decrease in I_{to} current density, and prolongation of APD. *CnAβ* gene knockdown significantly inhibited the effects of phenylephrine stimulation. Our data indicate that *CnAβ* gene knockdown can inhibit I_{to} channel remodeling and APD prolongation in hypertrophic neonatal rat ventricular myocytes. This finding suggests that calcineurin may be a potential target for the prevention of malignant ventricular arrhythmia in a hypertrophic heart.

Keywords: ventricular hypertrophy, transient outward potassium current, calcineurin, ion channel remodeling, action potential

1 Introduction

Ventricular remodeling caused by pathological cardiac hypertrophy is chronic congestive heart failure's most important pathophysiological mechanism [1,2]. Sudden cardiac death is the dominant reason of death in patients with congestive heart failure [3]. Ion channel remodeling in ventricular myocytes is the main pathophysiological basis leading to changes in the action potential duration (APD) of ventricular myocytes, resulting in malignant ventricular arrhythmia [4,5]. Congenitally, dysregulation of transient outward potassium current (I_{to}) has also been demonstrated to play a pivotal role in the Brugada syndrome [6,7].

I_{to} is a rapidly activated and inactivated outward potassium current, mainly involved in phase 1 of action potentials. The activity of I_{to} channels influences the activation of voltage-gated Ca^{2+} channels and the balance of inward and outward currents during the plateau, thereby mediating the duration and the amplitude of phase 2. In cultured hypertrophic ventricular myocytes, or the ventricular myocytes from a myocardial infarction heart, downregulated or dysfunctional I_{to} channels of ventricular myocytes lead to delayed repolarization and prolonged APD, which may easily cause fatal arrhythmia [8,9].

Calcineurin, a Ca^{2+}-calmodulin-regulated phosphatase, has been shown to participate in hypertrophic signal transduction. Research have shown that the continuous activation of calcineurin promotes cardiac hypertrophic remodeling, decompensated heart failure, and arrhythmic death [10,11]. Additionally, calcineurin regulates ion channel remodeling in hypertrophic cardiomyocytes [9,12–15].

# Contributed equally to this work.

*** Corresponding author: Long Yang,** Department of Cardiology, Guizhou Provincial People's Hospital, No. 83 Zhongshandong Road, Guiyang 550002, China, tel: +86-0851-8560-9229, fax: +86-0851-85924943, e-mail: yanglong1001@163.com
Na Deng: Department of Cardiology, The Affiliated Hospital of Guizhou Medical University, Guiyang 550025, China
Jionghong He, Guiling Xia, Ying Yang, Yidong Zhao, Zhaomei Huo, Chuxian Guo: Department of Cardiology, Guizhou Provincial People's Hospital, No. 83 Zhongshandong Road, Guiyang 550002, China

In transgenic mice, overexpression of calcineurin results in cardiac hypertrophy and the downregulation of I_{to}, which was reversed by the calcineurin inhibitor cyclosporine [13]. In rats after myocardial infarction, cyclosporine significantly attenuated the decreases in mRNA levels of Kv4.2 and Kv4.3, the components of α subunit in I_{to} channel, and I_{to} density in the left ventricular [14]. In cultured adult canine left ventricular cardiomyocytes, rapid pacing reduced I_{to} density and Kv4.3 mRNA and protein expression, which was markedly prevented by inhibiting calcineurin with cyclosporine [15]. Those results indicated that the activation of calcineurin may lead to I_{to} downregulation. Conversely, there was also evidence in cultured neonatal rat ventricular myocytes that the overexpression of constitutive calcineurin upregulates Kv4.2 expression without affecting Kv4.3 [9]. Thus, the precise role of calcineurin in the regulation of I_{to} remains unclear.

The purpose of this study is to clarify the regulatory effect of calcineurin on I_{to} channel remodeling and APD alterations in the hypertrophic ventricular myocytes of rats by way of knockdown of calcineurin-related genes.

2 Materials and methods

2.1 Materials

The Axopatch 700B patch clamp amplifier and Digidata 1322 data converter were from Axon (USA). The Sutter P-97 microelectrode puller was from Sutter (USA) and the BJ-40 glass microelectrode was from Beijing Zhengtianyi Electronics (China). Trypsin and collagenase (type II) were purchased from Sigma (USA). High-glucose Dulbecco's modified Eagle's medium (DMEM), premium fetal bovine serum (FBS), phenylephrine (PE), and 5-bromo-2-deoxyuridine (5-BrdU) were purchased from Gibco-BRL (USA). The following antibodies were used: rabbit anti-calcineurin Aβ (CnAβ) antibody (Merck Millipore, Germany), α striated muscle sarcomere actin (α-SCA) antibody (Sigma), horseradish peroxidase-conjugated anti-rabbit antibody (Santa Cruz, USA), rabbit anti-rat Kv4.2 antibody (Abcam, USA), and mouse-derived anti-rat glyceraldehyde-3-phosphate dehydrogenase (GAPDH) antibody (Shanghai Kangcheng Biotech, China). The Genomic DNA Purification Kit was purchased from Fermentas (Canada). The RNeasy Mini Kit was purchased from Qiagen (China). Ad-CnAβshRNA, the gene mediated by the recombinant adenovirus shRNA interference vector for silencing the A subunit β subtype of CaN, and the empty viral vector (null) were prepared by HanBio (Shanghai, China).

2.2 Isolation and culture of ventricular myocytes from neonatal rats

One-day-old neonatal Sprague-Dawley rats of clean grade were provided by the Animal Center of Peking University Health Science Center (license number: SYXK [Beijing] 2011-0039). The rats were sacrificed under anesthesia and the animals were fully immersed in 75% ethanol. The ventricle was harvested, the ventricular tissue was cut into small pieces, and the cells were isolated by enzymatic hydrolysis (final concentration of trypsin is 0.1%; the final concentration of type II collagenase is 0.03%). Ventricular myocytes were obtained by differential adherence and 5-BrdU affinity purification. The cells were cultured in high-glucose DMEM containing 10% FBS at 37°C in a 5% CO_2 incubator. After 48 h, the cells were cultured with serum-free DMEM with high glucose for the next experiment.

Ethical approval: The research related to animal use has complied with all the relevant national regulations and institutional policies for the care and use of animals and has been approved by the Ethics Committee of Guizhou Provincial People's Hospital (Hospital Ethics Review [2012] No. 001).

2.3 Identification of ventricular myocytes

Cells were cultured on fibrin-coated glass slides for 48 h and α-SCA was detected by immunofluorescence staining. Neonatal rat cardiac fibroblasts were used as a negative control (Figure A).

2.4 Ad-CnAβshRNA sequence screening

Primary ventricular myocytes were cultured for 48 h. Ad-CnAβshRNA1 (A1, interference base sequence 5′-3′: CAG AAAGGGTCTATGAAGCTTGTAT), Ad-CnAβshRNA2 (A2, interference base sequence 5′-3′: CCGCCAGTTTAACTGTT CTCCACAT), Ad-CnAβshRNA3 (A3, interference base sequence 5′-3′: GCAAGATGGCAAGAGTCTTCT), and null at a multiplicity of infection (MOI) of 50 were selected

to infect cultured ventricular myocytes for 48 h. CnAβ protein expression in the ventricular myocytes of each group was detected by western blotting. The Ad-CnAβshRNA corresponding to the lowest CnAβ protein expression was regarded as the optimal Ad-CnAβshRNA. A1 caused the most obvious decrease in CnAβ protein expression after its infection of ventricular myocytes at 48 h, and thus it was used in subsequent experiments (Figure A2).

2.5 Grouping and interventions

Ventricular myocytes were cultured for 48 h and then cultured in serum-free DMEM. These cells were divided into four groups. (1) In the null group, an adenovirus empty vector at an MOI of 50 was added. After 6 h of infection, the cells were cultured in two volumes of fresh serum-free DMEM for 48 h. (2) In the null + PE group, an adenovirus empty vector at an MOI of 50 was added. After 6 h of infection, the cells were cultured in two volumes of fresh serum-free DMEM with a total of 100 μM of PE (Gibco-BRL, USA) for 48 h. (3) In the A1 group, A1 at an MOI of 50 was added. After 6 h of infection, the cells were cultured in two volumes of fresh serum-free DMEM for 48 h. (4) In the A1 + PE group, A1 at an MOI of 50 was added. After 6 h of infection, the cells were cultured in two volumes of fresh serum-free DMEM with a total of 100 μM of PE for 48 h.

2.6 Determining the effectiveness of intervention on hypertrophy in cultured cells

Cell hypertrophy was identified by the measurement of *brain natriuretic peptide* (*BNP*) mRNA expression and cell size after 48 h of intervention. Upon completion of cell grouping and intervention, real-time reverse transcription-polymerase chain reaction (RT-PCR) was conducted to determine *BNP* mRNA expression in ventricular myocytes. Cells were cultured on glass slides. Crystal violet staining assay was performed after grouping and intervention. Three fields of view were randomly selected in each group. The surface area of the cells was assessed using Image J software.

2.7 RT-qPCR

Total RNA was extracted from ventricular myocytes using the RNeasy Mini Kit according to the manufacturer's instructions. A total of 1 μg of RNA was reverse transcribed using random hexamers from a first-strand cDNA synthesis kit. The mRNAs expression was measured by the real-time PCR method. The cycling conditions were as follows: 95°C for 10 min, followed by 40 cycles of 15 s at 95°C, and 30 s at 60°C. mRNA levels were normalized to GAPDH and determined using the 2-ΔΔCq method. Primers were designed using the Oligo 6.0 software. Specific primers were used to identify and amplify BNP (sense primer: 5′-GTCTCCAGAACAATCCACGA-3′; antisense primer: 5′-CTAAAACAACCTCAGCCCGT-3′), Kv4.2 (sense primer: 5′-GCTCTTCAGCAAGCAAGTTC-3′; antisense primer: 5′- TCC GACTGAAGTTAGACACG-3′), and *GAPDH* (sense primer: 5′- TGATGACATCAAGAAGGTGGTGAAG-3′; antisense primer: 5′- TCCTTGGAGGCCATGTAGGCCAT-3′).

2.8 Western blotting

Total protein (40 μg) was loaded and then transferred to a nitrocellulose membrane after electrophoresis. The membrane was blocked with 5% skim milk for 1 h. Rabbit anti-rat GAPDH antibody (1:1,000), rabbit anti-rat rabbit anti-CnAβ antibody (1:500), and rabbit anti-rat rabbit anti-rat Kv4.2 antibody (1:1,000) were added before overnight incubation at 4°C. After thorough rinsing, horseradish peroxidase-labeled secondary antibody was added for incubation at room temperature for 1 h. After thorough rinsing again, color development, photography, and quantitative measurement of the gray scale were performed.

2.9 Whole-cell patch clamp detection

A glass microelectrode formed a high resistance seal with the cells and ruptured the membrane. I_{to} was recorded under the voltage clamp mode. Current density analysis was used (current density [pA/pF] = current intensity/capacitance) to avoid errors caused by cell size. The action potential of the individual cells was recorded under the current clamp mode. The current signal was guided by an Ag/AgCl electrode, amplified by a patch clamp AXON 700B amplifier through an AD/DA converter board, and stored in a computer hard disk. During the experimental procedure, stimulation discharge and signal acquisition were controlled by pCLAMP 10.0 software.

In the I_{to} depolarization step, the clamping voltage was set to −80 mV with an −40 mV to +70 mV pulse stimulation series, with a step voltage of 10 mV, wave width of 300 ms, and frequency of 0.2 Hz. The I_{to} steady-state

activation curve stimulation protocol was as follows. The clamping voltage was set to −80 mV with a −40 to + 70 mV pulse stimulation series, with a step voltage of 10 mV and a wave width of 300 ms. The I_{to} current was then recorded. The I_{to} steady-state inactivation curve stimulation protocol was as follows. The clamping voltage was set to −80 mV with a −40 mV to +50 mV pulse stimulation series, with a step voltage of 10 mV and a wave width of 1,000 ms. The residual current was then recorded. The steady-state activation and inactivation curves were created using the normalized current values obtained by the two above-mentioned stimulation schemes as the ordinate and the stimulation pulses under different voltages as the abscissa. The semi-activated voltage ($V_{1/2,act}$) and semi-inactivated voltage ($V_{1/2,inact}$) were calculated by curve fitting using the Boltzmann equation ($I/I_{max} = 1/\{1 + \exp[(V_{1/2} - V_m)/k]\}$).

The action potential recording method was similar to the voltage clamp mode. After membrane sealing, membrane breaking, and compensation, the recording was switched to the current clamp mode. A 1 nA current pulse was then applied, with a wave width of 2.5 ms, which induced the action potential in the ventricular myocytes. The APDs at 20, 50, and 90% repolarization (APD20, APD50, and APD90) were recorded and analyzed.

2.10 Statistical analysis

Statistical analysis was performed using the Graphpad Prism 6 software. All data are expressed as mean ± SD. Differences among groups were compared by one-way analysis of variance, and the *q* test was used for comparison of the two groups. A *P* value of <0.05 was considered statistically significant.

3 Results

3.1 Effectiveness of stimulation on *BNP* mRNA expression and the surface area of ventricular myocyte

In the null + PE group, PE treatment for 48 h significantly upregulated *BNP* mRNA expression by an average of 2.24 times ($P < 0.01$), and significantly increased the surface area ((1,360 ± 90) μm^2 vs (700 ± 40) μm^2, $P < 0.01$) of ventricular myocytes compared with the null group. Therefore, PE intervention led to hypertrophy of ventricular myocytes. The *BNP* mRNA expression in the A1 + PE group was markedly attenuated compared with that in the null + PE group (1.15 ± 0.09 vs 2.24 ± 0.48, $P < 0.05$), as well as the surface area of cells ((680 ± 180) μm^2 vs (1,360 ± 90) μm^2, $P < 0.01$), indicating that the cellular hypertrophy induced by PE was significantly inhibited by Ad-CnAβshRNA intervention (Figures 1 and 2, and Table 1).

3.2 Effect of Ad-CnAβshRNA intervention on PE-induced CnAβ protein expression in ventricular myocytes

In the null + PE group, PE treatment significantly upregulated CnAβ protein expression by an average of 2.29 times ($P < 0.01$) when compared with the null group. In contrast, CnAβ protein expression was significantly lower in the A1 + PE group than in the null + PE group (0.90 ± 0.12 vs 2.29 ± 0.24, $P < 0.01$) (Figure 3 and Table 1).

3.3 Effect of Ad-CnAβshRNA intervention on PE-induced *Kv4.2* mRNA and protein expression in ventricular myocytes

In the null + PE group, PE treatment significantly downregulated *Kv4.2* mRNA (1 vs 0.62 ± 0.07, $P < 0.05$) and

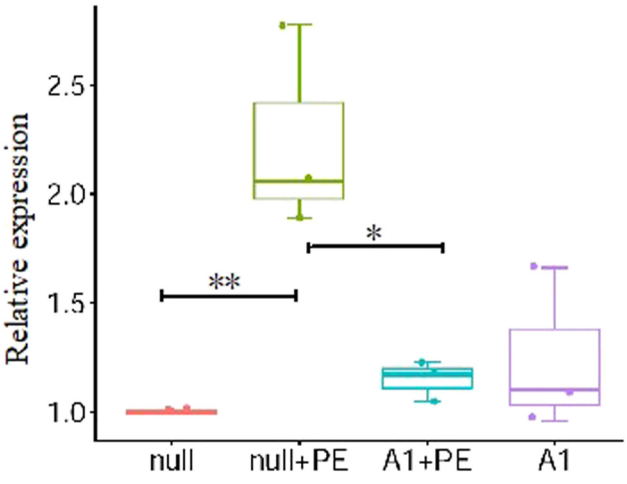

Figure 1: PE stimulation promoted the *BNP* mRNA expression in ventricular myocytes which was attenuated by pre-treatment with Ad-CnAβshRNA1. Bar chart showed the quantitative analysis results of *BNP* mRNA by real-time reverse transcription-polymerase chain reaction. *$P < 0.05$; $n = 3$. PE: Phenylephrine. A1: Ad-CnAβshRNA.

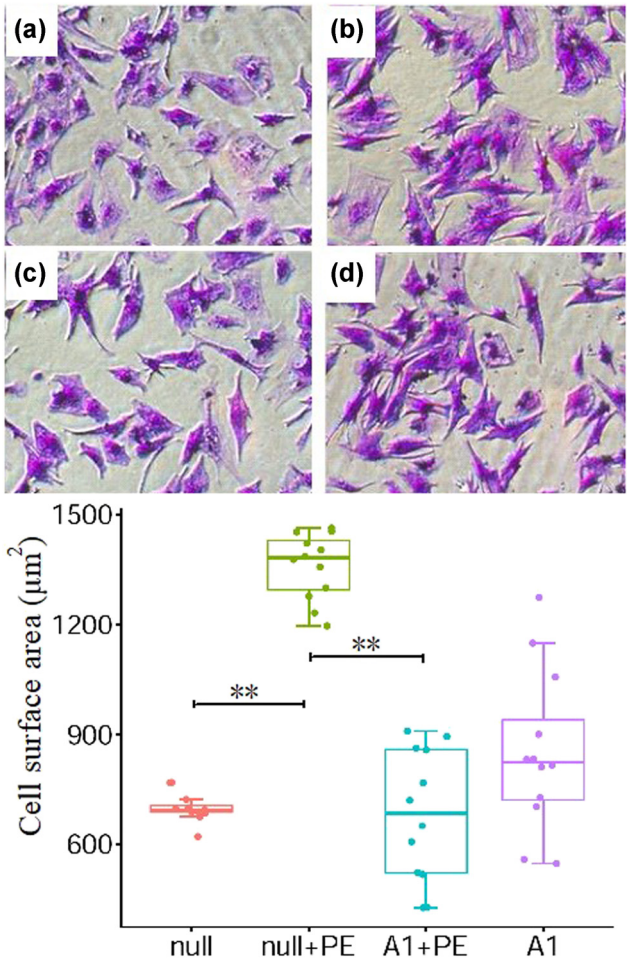

Figure 2: PE stimulation promoted cell hypertrophy which was attenuated by pre-treatment with Ad-CnAβshRNA1. Color picture showed the ventricular cells stained with crystal violet in four groups. a, b, c, and d are the null, null + PE, A1 + PE, and A1 groups, respectively (×100). The histogram showed the comparative results of cell area in groups. *$P < 0.05$, **$P < 0.01$. PE: Phenylephrine. A1: Ad-CnAβshRNA.

protein (1 vs 0.58 ± 0.11, $P < 0.05$) expression when compared to the null group. In contrast, *Kv4.2* mRNA (1.35 ± 0.18 vs 0.62 ± 0.07, $P < 0.01$) and protein (0.88 ± 0.09 vs 0.58 ± 0.11, $P < 0.05$) expression was significantly higher in the A1 + PE group than in the null + PE group (Figure 4 and Table 1).

3.4 Effect of Ad-CnAβshRNA intervention on I_{to} in ventricular myocytes

At a stimulation voltage of +20 to +70 mV, I_{to} current density in the null + PE group was significantly lower than that in the null group (Table 2), the averaged current–voltage (I–V) curve relations of I_{to} remarkably shifted downward, and the peak current density was decreased by 49% ($P < 0.05$; Figure 5). The A1 + PE group had significantly higher I_{to} current density than the null + PE group ($P < 0.05$; Figure 5 and Table 2). The shape and distribution of the activation curves of I_{to} were similar among the different groups (Figure 6a), and the $V_{1/2,act}$ showed no significant difference among the groups ($P > 0.05$; Figure 6b and Table 3). The inactivation curve of I_{to} was significantly shifted to the left in the null + PE group when compared with the null group and was significantly shifted to the right in the A1 + PE group compared to the null + PE group (Figure 6c). The $V_{1/2,inact}$ was significantly lower in the null + PE group than in the null group ($P < 0.05$) and significantly higher in the A1 + PE group than in the null + PE group ($P < 0.05$; Figure 6d and Table 3). Therefore, stimulation of ventricular myocytes with PE accelerated the inactivation of I_{to}, whereas Ad-CnAβshRNA1 intervention inhibited such an effect.

3.5 Effect of Ad-CnAβshRNA intervention on APD in ventricular myocytes

APD20, APD50, and APD90 were significantly longer in the null + PE group than in the null group and were

Table 1: Comparison of the expression of mRNAs and proteins, and the cell area in each group ($\overline{x} \pm s$)

	n	Null	Null + PE	A1 + PE	A1
BNP mRNA	3	1**	2.24 ± 0.48	1.15 ± 0.09*	1.24 ± 0.37
Cell area (μm²)	12	700 ± 40**	1360 ± 90	680 ± 180**	850 ± 220
CnAβ protein	3	1**	2.29 ± 0.24	0.90 ± 0.12**	1.18 ± 0.07
Kv4.2 mRNA	5	1*	0.62 ± 0.07	1.35 ± 0.18**	1.2 ± 0.21
Kv4.2 protein	4	1*	0.58 ± 0.11	0.88 ± 0.09*	1.05 ± 0.2

The expression of mRNAs and proteins were exhibited as relative data. Compared with null + PE group, *$P < 0.05$, **$P < 0.01$. PE: phenylephrine. A1: Ad-CnAβshRNA. *BNP*: brain natriuretic peptide. CnAβ: calcineurin Aβ.

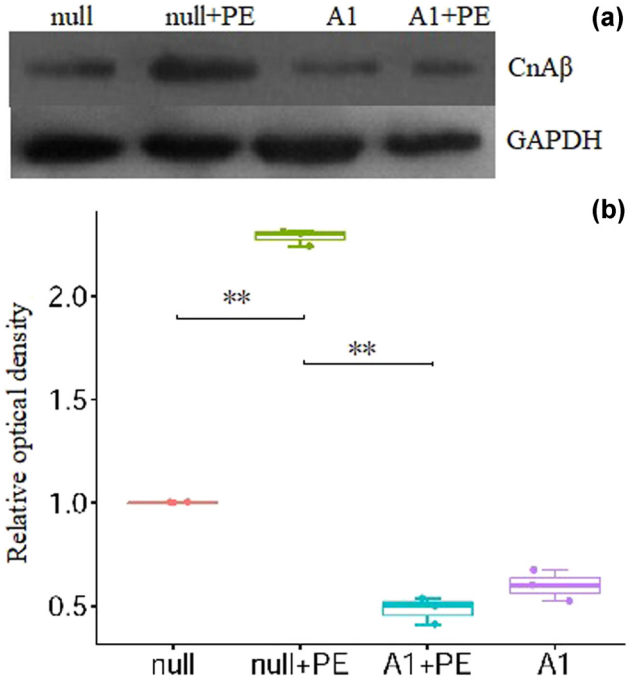

Figure 3: PE stimulation increased CnAβ protein expression which was attenuated by pre-treatment with Ad-CnAβshRNA1. (a) The representative picture of CnAβ protein detected by Western blotting. (b) The semiquantitative analysis results of CnAβ protein in groups. $^{**}P < 0.01$, $n = 3$. CnAβ: Calcineurin Aβ. PE: Phenylephrine. A1: Ad-CnAβshRNA.

significantly shorter in the A1 + PE group than in the null + PE group (Figure 7 and Table 4). Therefore, PE intervention led to significant prolongation of APD in ventricular myocytes, whereas Ad-CnAβshRNA intervention attenuated such an effect.

4 Discussion

The reduction of I_{to} slows the repolarization of the action potential in the first phase and reduces the depth of the phase 1 notch, thus affecting the activity of other ion channels. The Kv4.3 channel is expressed in human left ventricular muscle and shows a gradient of protein across the ventricular wall, thus forming electrophysiological transmural heterogeneity [16,17]. In the hypertrophic ventricular myocardium in animal models of cardiac hypertrophy or patients with organic heart disease, especially in patients with co-existing heart failure and myocardial injury, the expression of Kv4.3 and Kv4.2 in ventricular myocytes is downregulated and the activity of I_{to} channels is reduced. This leads to abnormal early repolarization, repolarization delay, and APD prolongation, which may easily cause fatal ventricular arrhythmias [8,9,18,19].

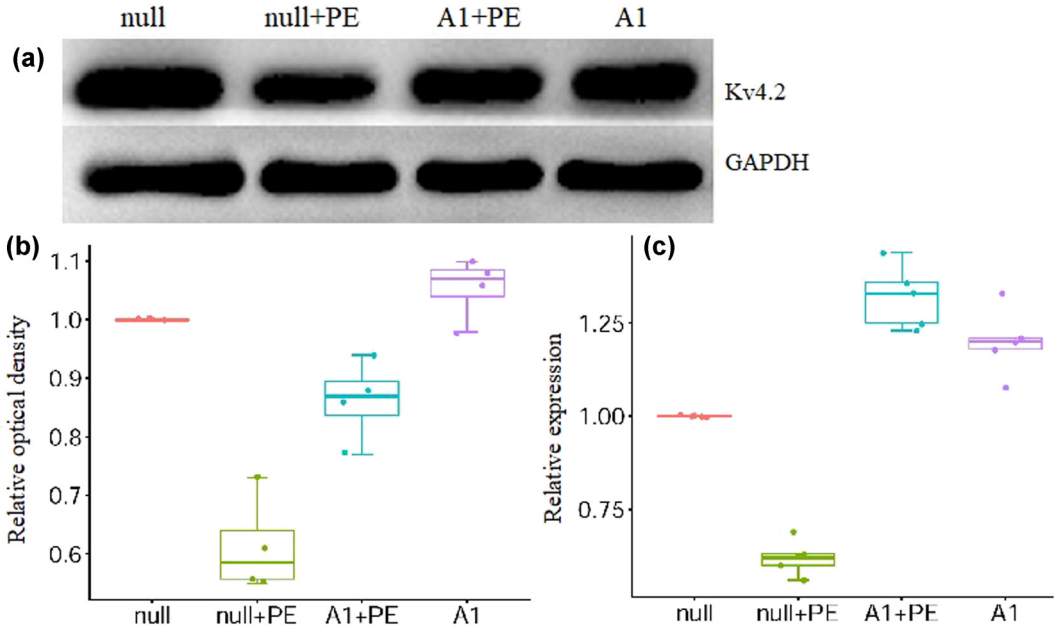

Figure 4: PE intervention inhibited the protein and mRNA expression of Kv4.2 which was attenuated by pre-treatment with Ad-CnAβshRNA1. (a) The representative picture of Kv4.2 protein detected by western blotting. (b and c) The semiquantitative analysis results of Kv4.2 protein ($n = 4$) and mRNA ($n = 5$) in groups, respectively. $^{*}P < 0.05$, $^{**}P < 0.01$. PE: Phenylephrine. A1: Ad-CnAβshRNA.

Table 2: Comparison of current densities (pA/pF) at different voltages in each group ($\bar{x} \pm s$)

	n	20 mV	30 mV	40 mV	50 mV	60 mV	70 mV
Null	14	7.83 ± 1.04	11.03 ± 1.15	14.28 ± 1.22	17.48 ± 1.45	20.99 ± 1.76	24.02 ± 1.86
Null + PE	12	5.04 ± 1.24	6.27 ± 1.18	7.80 ± 1.21	9.10 ± 1.25	10.89 ± 1.51	12.27 ± 1.88
A1 + PE	12	6.38 ± 0.79	8.45 ± 0.79	10.46 ± 0.88	12.33 ± 1.12	14.65 ± 1.24	16.85 ± 1.38
A1	12	7.41 ± 1.10	9.86 ± 1.06	12.76 ± 0.86	15.38 ± 0.51	18.51 ± 0.64	21.15 ± 0.89

At a stimulation voltage of 20–70 mV: null vs null + PE, $P < 0.05$; A1 + PE vs null + PE, $P < 0.05$. PE: phenylephrine. A1: Ad-CnAβshRNA.

The molecular structure of the I_{to} ion channel includes a pore-forming α subunit and an auxiliary β subunit. The α subunit of I_{to} channel has two functionally distinct components. The fast component, $I_{to,fast}$ ($I_{to,f}$), for example, recovers from inactivation very rapidly with time constants in the range of 60–100 ms [20,21]. In contrast, the slow component, $I_{to,slow}$ ($I_{to,s}$), recovers from inactivation slowly with time constants on the order of seconds [22,23]. Usually, I_{to} is referred to the $I_{to,fast}$. The fast component of α subunit is formed by assembly of Kv4.2 subunits, Kv4.3 subunits, or a combination of the two, which shows the heterogeneity of the species and the different regions of the same heart [23–27].

Selective gene silencing using antisense oligonucleotides (AsODNs) targeted against Kv4.2 and Kv4.3 reduced $I_{to,f}$ in cultured rodent ventricular myocytes [28,29]. In rat atrial myocytes, AsODNs targeted against Kv4.2, but not Kv4.3, attenuated $I_{to,f}$ [30], whereas in human atrial myocytes, $I_{to,f}$ was significantly attenuated by Kv4.3, but not by Kv4.2 and AsODNs [31]. In addition, targeted gene deletion of Kv4.2 in mice eliminates ventricular $I_{to,f}$, further revealing the critical role of Kv4.2 in the generation of $I_{to,f}$ channels in rodents [32]. So, in this study, Kv4.2 was chosen as the research component of I_{to} channel other than Kv4.3.

Ventricular hypertrophy is an effective compensation for chronic heart overload, but eventually develops into congestive heart failure because of decompensation following ventricular remodeling [1,2]. Remodeling of numerous ion channels in ventricular myocytes during this process is an important basis for malignant ventricular arrhythmias. Many cell signaling factors are involved in regulating ion channel remodeling in hypertrophic cardiomyocytes. Promoting *calcineurin* mRNA and protein expression and enhancing calcineurin activity can promote hypertrophy of cardiomyocytes and participate in regulating multiple ion channel remodeling in cardiomyocytes [10,12,13,29]. In rat models of myocardial infarction, the calcineurin inhibitor cyclosporin A can significantly inhibit ventricular remodeling and hypertrophy, improve diastolic function, inhibit a decrease in I_{to} current density in ventricular myocytes, and downregulate *Kv4.2* and *Kv4.3* mRNA and protein expression [14]. In ventricular myocytes of mouse myocardial infarction models, I_{to} current density is decreased, and *Kv4.2* and *Kv4.3* mRNA and protein expression is downregulated [8]. Furthermore, the β-blocker metoprolol, the calcineurin inhibitor cyclosporin

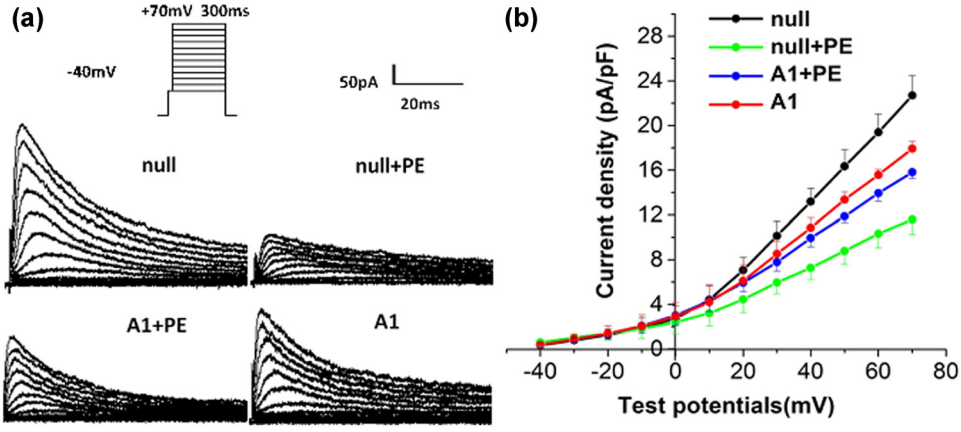

Figure 5: Densities of transient outward potassium current (I_{to}) in ventricular myocytes. (a) A typical I_{to} recording from isolated ventricular myocytes in groups. (b) Current–voltage (I–V) curve relations. At a stimulation voltage of +20 to +70 mV, PE intervention significantly decreased I_{to} density ($P < 0.05$), which was markedly attenuated by pre-treatment with Ad-CnAβshRNA1 ($P < 0.05$; the cell numbers are 14, 12, 12, and 12 in null, null + PE, A1 + PE and A1 groups, respectively). PE: Phenylephrine. A1: Ad-CnAβshRNA.

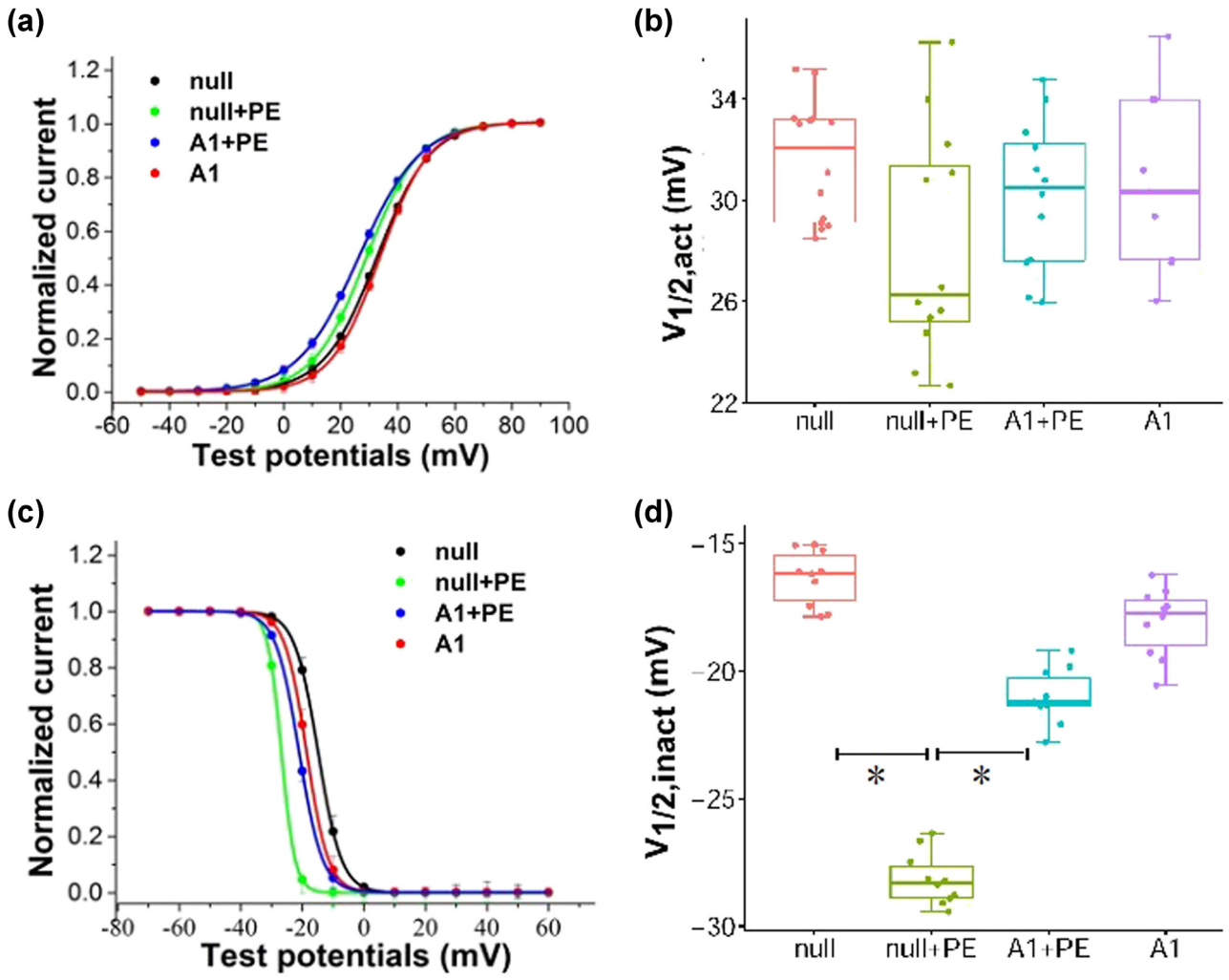

Figure 6: The activation and inactivation curves of transient outward potassium current (I_{to}). (a) The steady-state activation curve of I_{to}. (b) The semi-activated voltage ($V_{1/2,act}$) of I_{to}. There were no significant differences of $V_{1/2,\ act}$ among groups ($P > 0.05$; the cell numbers are 14, 12, 12, and 9 in null, null + PE, A1 + PE, and A1 groups, respectively). (c) The steady-state inactivation curve of I_{to}. (d) The semi-inactivated voltage ($V_{1/2,inact}$) of I_{to}. PE stimulation accelerated inactivation of I_{to}, which was inhibited by Ad-CnAβshRNA1 intervention (*$P < 0.05$; $n = 10$ in each group). PE: Phenylephrine. A1: Ad-CnAβshRNA.

Table 3: Comparison of $V_{1/2}$ of the activation curves and inactivation curves in each group ($\overline{x} \pm s$)

	n_{act}	$V_{1/2,act}$ (mV)	n_{inact}	$V_{1/2,inact}$ (mV)
Null	14	31.57 ± 2.38	10	−16.34 ± 1.07
Null + PE	12	28.21 ± 4.47	10	−28.15 ± 1.00*
A1 + PE	12	30.21 ± 2.91	10	−21.01 ± 1.07
A1	9	30.72 ± 3.51	10	−18.07 ± 1.34

Compared with null group or A1 + PE group, *$P < 0.05$. PE: phenylephrine.

A1: Ad-CnAβshRNA. $V_{1/2,act}$: semi-activated voltage. $V_{1/2,\ inact}$: semi-inactivated voltage.

n_{act} and n_{inact}: cell number in each group enrolled testing of $V_{1/2,act}$ or $V_{1/2,inact}$.

A, and knockout of calcineurin-specific downstream signaling factors (i.e., *NFAT4* gene, a member of the nuclear factor of activated T cells [NFAT] family) can significantly inhibit a decrease in I_{to} current density and inhibit changes in *Kv4.2* and *Kv4.3* mRNA and protein expression. In hypertrophic neonatal rat cardiomyocytes, activation of the calcineurin-NFAT signal upregulates the transcriptional expression of *Kv4.2* mRNA and protein and increases I_{to} current density [9]. In canine ventricular myocytes with simulated ventricular tachycardia, *Kv4.3* mRNA and protein expression is downregulated, and I_{to} current density is significantly reduced, which manifests as significant inhibition of cyclosporine [15].

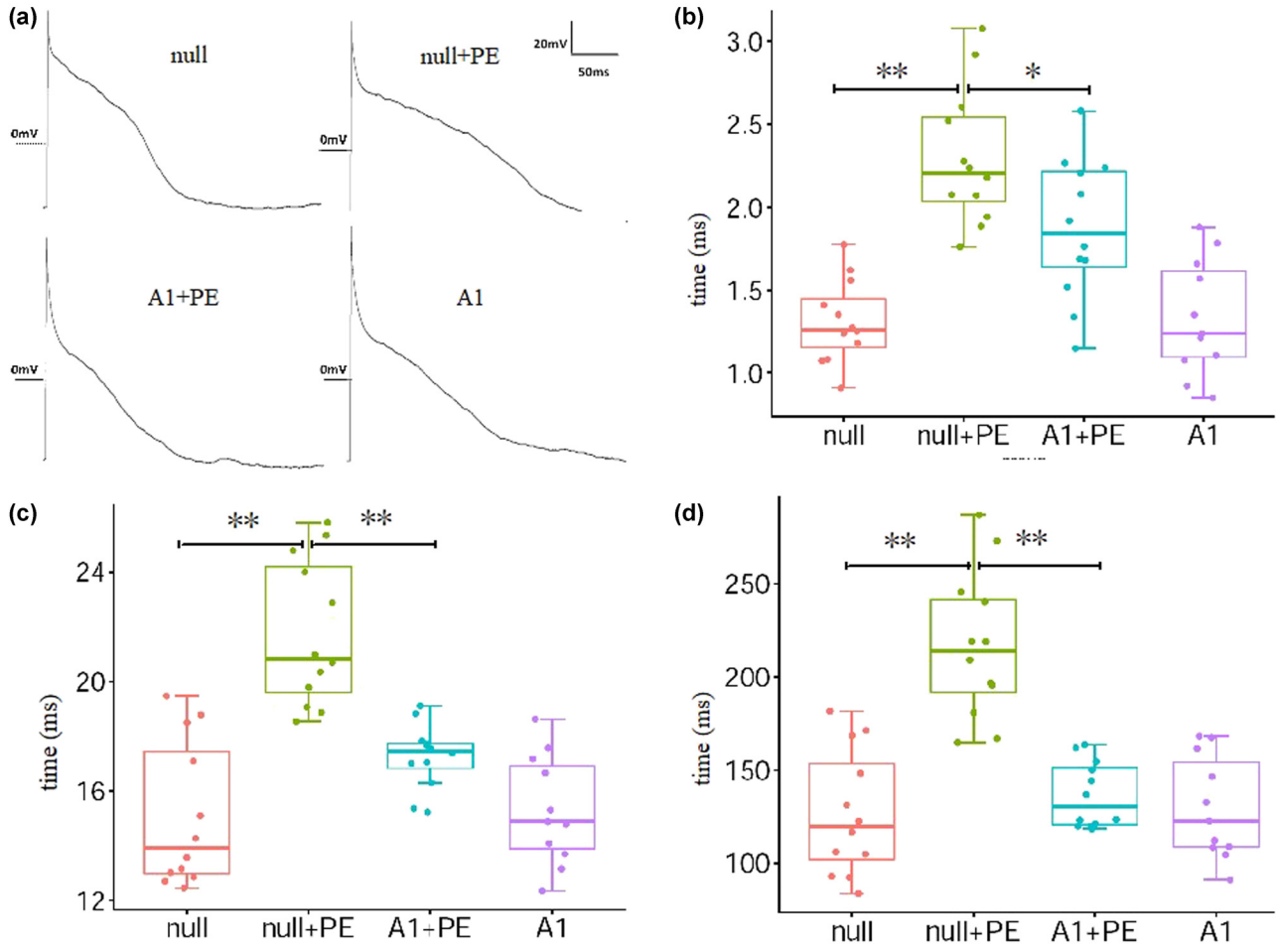

Figure 7: Action potentials of ventricular myocytes. (a) Representative action potentials of cultured ventricular myocytes. (b–d) The analysis results of the APD20, APD50, and APD90 in groups. PE stimulation prolonged the APD, which was inhibited by Ad-CnAβshRNA1 intervention. $^{**}P < 0.001$, $^{*}P < 0.05$; the cell numbers are 12, 12, 12, and 11 in null, null + PE, A1 + PE, and A1 groups, respectively. PE: Phenylephrine. A1: Ad-CnAβshRNA.

Table 4: Comparison of APD (ms) in each group ($\overline{x} \pm s$)

	n	APD_{20}	APD_{50}	APD_{90}
Null	12	1.31 ± 0.26**	15.08 ± 2.65**	126.66 ± 35.55**
Null + PE	12	2.30 ± 0.41	21.75 ± 3.24	216.44 ± 39.43
A1 + PE	12	1.87 ± 0.42*	17.25 ± 1.19**	136.41 ± 17.66**
A1	11	1.33 ± 0.35	15.30 ± 1.98	129.48 ± 27.51

Compared with null group or A1 + PE group, $^{*}P < 0.05$, $^{**}P < 0.01$. PE: phenylephrine, A1: Ad-CnAβshRNA. APD: action potential duration.

In this study, the knockdown of the *CnAβ* gene, which encoded the main functional unit of calcineurin, completely inhibited CnAβ protein expression, which defected in the substance base that enables calcineurin to function. Therefore, we evaluated the effect of completely suppressed calcineurin activity on I_{to}. When the stimulation voltage was between +20 and +70 mV, intervention with the conventional α_1 adrenergic receptor agonist PE significantly reduced I_{to} current density in the ventricular myocytes of neonatal rats. The peak current density decreased by 49%, and the *I–V* curves of I_{to} remarkably shifted downward. Furthermore, APD20, APD50, and APD90 were significantly prolonged. Knockdown of the *CnAβ* gene significantly inhibited the effect of PE intervention on I_{to} current density and APD. Moreover, PE stimulation did not affect the activation of I_{to}, but PE reduced I_{to} current density by accelerating its inactivation. Additionally, the knockdown of the *CnAβ* gene inhibited the effect of PE on I_{to} inactivation.

The results of earlier studies showed that the precise role of calcineurin in the regulation of I_{to} remains unclear [9,13–15]. In those studies, calcineurin activity was promoted by the agonist or transgenic method, and was

depressed by cyclosporine [9,13–15]. As per our knowledge, this study is the first one to assess the role of calcineurin in the regulation of I_{to} by way of calcineurin gene silence. Our results potently showed that calcineurin is a negative regulator of I_{to} activity in ventricular myocytes from neonatal rats.

In summary, our findings indicated that *CnAβ* gene knockdown can inhibit PE-induced I_{to} channel remodeling and APD prolongation in hypertrophic neonatal rat ventricular myocytes. This finding suggested that calcineurin may be a potential target for the prevention of malignant ventricular arrhythmia in hypertrophic hearts. However, the study had some limitations. Many ion channels are involved in the formation of action potential in ventricular myocytes. However, this study only detected the I_{to} ion channel. Moreover, as one of the coding genes of I_{to} ion channel, the expression of Kv4.3 was not detected.

Funding information: This study was supported by the Guizhou Provincial Science and Technology Fund (Grant No. (2019) 1205), and the Clinical Research Center Project of the Department of Science and Technology of Guizhou Province (NO. (2017)5405).

Author contributions: Long Yang, Na Deng, and Jionghong He designed the research and carried out the experiment. Na Deng and Jionghong He completed data analysis and manuscript writing. Long yang completed the final revision and finalization of the manuscript. Guiling Xia, Ying Yang, Yidong Zhao, Zhaomei Huo, and Chuxian Guo participated in the experiment in varying degrees.

Conflict of interest: The authors state no conflict of interest.

Data availability statement: The datasets generated during and/or analyzed during the current study are available from the corresponding author on reasonable request.

References

[1] Oldfield CJ, Duhamel TA, Dhalla NS. Mechanisms for the transition from physiological to pathological cardiac hypertrophy. Can J Physiol Pharmacol. 2020;98(2):74–84.

[2] Shimizu I, Minamino T. Physiological and pathological cardiac hypertrophy. J Mol Cell Cardiol. 2016;97:245–62.

[3] Huang D, Hua W, Fang Q, Yan J, Su Y, Liu B, et al. POSCD-China Biventricular pacemaker and defibrillator implantation in patients with chronic heart failure in China. ESC Heart Fail. 2021;8(1):546–54.

[4] Wang Y, Hill JA. Electrophysiological remodeling in heart failure. J Mol Cell Cardiol. 2010;48(4):619–32.

[5] Kepenek ES, Ozcinar E, Tuncay E, Akcali KC, Akar AR, Turan B. Differential expression of genes participating in cardiomyocyte electrophysiological remodeling via membrane ionic mechanisms and Ca^{2+}-handling in human heart failure. Mol Cell Biochem. 2020;463(1–2):33–44.

[6] David JP, Lisewski U, Crump SM, Jepps TA, Bocksteins E, Wilck N, et al. Deletion in mice of X-linked, Brugada syndrome- and atrial fibrillation-associated Kcne5 augments ventricular K V currents and predisposes to ventricular arrhythmia. FASEB J. 2019;33(2):2537–52.

[7] Portero V, Le Scouarnec S, Es-Salah-Lamoureux Z, Burel S, Gourraud JB, Bonnaud S, et al. Dysfunction of the voltage-gated K^+ channel β_2 subunit in a familial case of Brugada syndrome. J Am Heart Assoc. 2016;5(6):e003122.

[8] Rossow CF, Minami E, Chase EG, Murry CE, Santana LF. NFATc3-induced reductions in voltage-gated K^+ currents after myocardial infarction. Circ Res. 2004;94(10):1340–50.

[9] Gong N, Bodi I, Zobel C, Schwartz A, Molkentin JD, Backx PH. Calcineurin increases cardiac transient outward K^+ currents via transcriptional up-regulation of Kv4.2 channel subunits. J Biol Chem. 2006;281(50):38498–506.

[10] Molkentin JD, Lu JR, Antos CL, Markham B, Richardson J, Robbins J, et al. A calcineurin-dependent transcriptional pathway for cardiac hypertrophy. Cell. 1998;93(2):215–28.

[11] Gao L, Liu Y, Guo S, Xiao L, Liang C, Wang X. Testin protects against cardiac hypertrophy by targeting a calcineurin-dependent signalling pathway. J Cell Mol Med. 2019;23(1):328–39.

[12] He J, Xu Y, Yang L, Xia G, Deng N, Yang Y, et al. Regulation of inward rectifier potassium current ionic channel remodeling by AT1-Calcineurin-NFAT signaling pathway in stretch-induced hypertrophic atrial myocytes. Cell Biol Int. 2018;42(9):1149–59.

[13] Dong D, Duan Y, Guo J, Roach DE, Swirp SL, Wang L, et al. Overexpression of calcineurin in mouse causes sudden cardiac death associated with decreased density of K^+ channels. Cardiovasc Res. 2003;57(2):320–32.

[14] Deng L, Huang B, Qin D, Ganguly K, El-Sherif N. Calcineurin inhibition ameliorates structural, contractile, and electrophysiologic consequences of postinfarction remodeling. J Cardiovasc Electrophysiol. 2001;12(9):1055–61.

[15] Xiao L, Coutu P, Villeneuve LR, Tadevosyan A, Maguy A, Le Bouter S, et al. Mechanisms underlying rate-dependent remodeling of transient outward potassium current in canine ventricular myocytes. Circ Res. 2008;103(7):733–42.

[16] Niwa N, Nerbonne JM. Molecular determinants of cardiac transient outward potassium current (*I*(to)) expression and regulation. J Mol Cell Cardiol. 2010;48(1):12–25.

[17] Wickenden AD, Kaprielian R, Kassiri Z, Tsoporis JN, Tsushima R, Fishman GI, et al. The role of action potential prolongation and altered intracellular calcium handling in the pathogenesis of heart failure. Cardiovasc Res. 1998;37(2):312–23.

[18] Guo Y, Zhang C, Ye T, Chen X, Liu X, Chen X, et al. Pinocembrin ameliorates arrhythmias in rats with chronic ischaemic heart failure. Ann Med. 2021;53(1):830–40.

[19] Taigen T, De Windt LJ, Lim HW, Molkentin JD. Targeted inhibition of calcineurin prevents agonist-induced cardiomyocyte hypertrophy. Proc Natl Acad Sci USA. 2000;97(3):1196–201.
[20] Patel SP, Campbell DL. Transient outward potassium current, 'I_{to}', phenotypes in the mammalian left ventricle: underlying molecular, cellular and biophysical mechanisms. J Physiol. 2005;569(Pt 1):7–39.
[21] Oudit GY, Kassiri Z, Sah R, Ramirez RJ, Zobel C, Backx PH. The molecular physiology of the cardiac transient outward potassium current (I_{to}) in normal and diseased myocardium. J Mol Cell Cardiol. 2001;33(5):851–72.
[22] Xu H, Guo W, Nerbonne JM. Four kinetically distinct depolarization-activated K^+ currents in adult mouse ventricular myocytes. J Gen Physiol. 1999;113(5):661–78.
[23] Brahmajothi MV, Campbell DL, Rasmusson RL, Morales MJ, Trimmer JS, Nerbonne JM, et al. Distinct transient outward potassium current (I_{to}) phenotypes and distribution of fast inactivating potassium channel α subunits in ferret left ventricular myocytes. J Gen Physiol. 1999;113(4):581–600.
[24] Alday A, Ahyayauch H, Fernández-López V, Echeazarra L, Urrutia J, Casis O, et al. CaMKIi modulates the cardiac transient outward K^+ current through its association with Kv4 channels in non-caveolar membrane rafts. Cell Physiol Biochem. 2020;54(1):27–39.
[25] Li X, Xue YM, Guo HM, Deng CY, Peng DW, Yang H, et al. High hydrostatic pressure induces atrial electrical remodeling through upregulation of inflammatory cytokines. Life Sci. 2020;242:117209.
[26] Gaborit N, Le Bouter S, Szuts V, Varro A, Escande D, Nattel S, et al. Regional and tissue specific transcript signatures of ion channel genes in the non-diseased human heart. J Physiol. 2007;582(Pt 2):675–93.
[27] Dixon JE, McKinnon D. Quantitative analysis of potassium channel mRNA expression in atrial and ventricular muscle of rats. Circ Res. 1994;75(2):252–60.
[28] Fiset C, Clark RB, Shimoni Y, Giles WR. Shal-type channels contribute to the Ca^{2+}-independent transient outward K^+ current in rat ventricle. J Physiol. 1997;500(Pt 1):51–64.
[29] Guo W, Li H, Aimond F, Johns DC, Rhodes KJ, Trimmer JS, et al. Role of heteromultimers in the generation of myocardial transient outward K^+ currents. Circ Res. 2002;90(5):586–93.
[30] Xu H, Li H, Nerbonne JM. Elimination of the transient outward current and action potential prolongation in mouse atrial myocytes expressing a dominant negative Kv4 α subunit. J Physiol. 1999;519(Pt 1):11–21.
[31] Wang Z, Feng J, Shi H, Pond A, Nerbonne JM, Nattel S. Potential molecular basis of different physiological properties of the transient outward K^+ current in rabbit and human atrial myocytes. Circ Res. 1999;84(5):551–61.
[32] Guo W, Jung WE, Marionneau C, Aimond F, Xu H, Yamada KA, et al. Targeted deletion of Kv4.2 eliminates $I_{to,f}$ and results in electrical and molecular remodeling, with no evidence of ventricular hypertrophy or myocardial dysfunction. Circ Res. 2005;97(12):1342–50.

Appendix

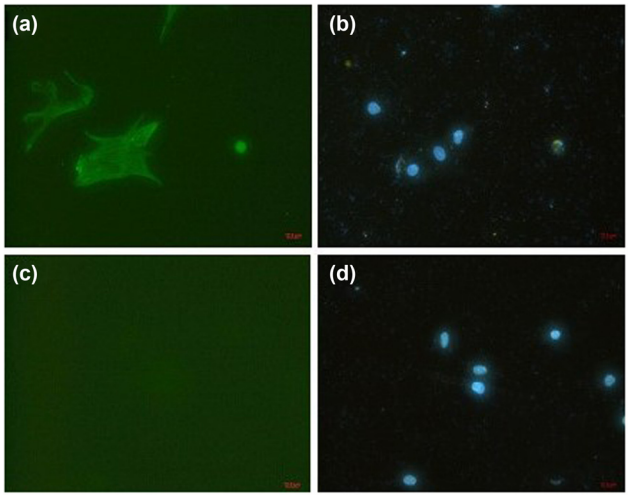

Figure A: Identification of ventricular myocytes. After 48 h of culture, myocardial cells were demonstrated by immunofluorescent staining with α striated muscle sarcomere actin (α-SCA) antibody that is specialized to striated muscle. (a) Cells appearing green were identified as myocardial cells. (c) Staining for fibroblasts was negative. (b and d) The blue was nuclei stained with diamidine phenylindole. Panels (a) and (b), (c), and (d) are the same view, respectively (×200).

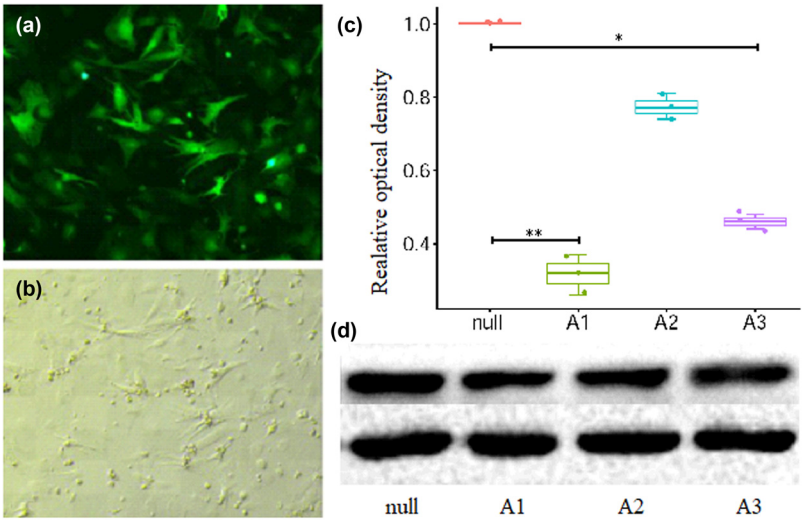

Figure A2: The results of Ad-CnAβshRNA sequence screening. A1 caused the most obvious decrease in the A subunit β subtype of calcineurin (CnAβ) protein expression after its infection of ventricular myocytes for 48 h. (a) Cells appearing green were identified as cells infected by recombinant adenovirus. (b) The photo taken in bright background at the same view of (a). (c) The semiquantitative analysis results of CnAβ protein. *$P < 0.05$, **$P < 0.01$; $n = 3$. (d) The representative picture of CnAβ protein detected by western blotting. A1: Ad-CnAβshRNA1. A2: Ad-CnAβshRNA2. A3: Ad-CnAβshRNA3.